Journal of Zhejiang University-SCIENCE A (Applied Physics & Engineering)
ISSN 1673-565X (Print); ISSN 1862-1775 (Online)
www.zju.edu.cn/jzus; www.springerlink.com
E-mail: jzus@zju.edu.cn

Supersonic mixing augmentation mechanism induced by a wall-mounted cavity configuration*

Wei HUANG†[1], Ming-hui LI[2], Feng DING[1], Jun LIU[1]

([1]*Science and Technology on Scramjet Laboratory, National University of Defense Technology, Changsha 410073, China*)

([2]*China Aerodynamics R&D Center, Mianyang 621000, China*)

†E-mail: gladrain2001@163.com

Received Sept. 5, 2015; Revision accepted Nov. 20, 2015; Crosschecked Dec. 16, 2015

Abstract: An efficient mixing process is very important for the engineering implementation of an airbreathing propulsion system. The air and injectant should be mixed sufficiently before entering the combustor. Two new wall-mounted cavity configurations were proposed to enhance the mixing process in a conventional transverse injection flow field. Their flow field properties were compared with those of a system with only transverse injection ports. Grid independency analysis was used to choose a suitable grid scale, and the mixing efficiencies at four cross-sectional planes (namely x=20, 40, 60, and 80 mm, which are just downstream of the jet orifice) were compared for the configurations considered in this study. The results showed that hydrogen penetrated deeper when a cavity was mounted upstream of the transverse injection ports. This is beneficial to the mixing process in supersonic flows. The mixing efficiency of the configuration with the wall-mounted cavity was better than that of the conventional physical model, and the mixing efficiency of the proposed novel physical model I (98.71% at x=20 mm) was the highest of all. In the case with only transverse injection ports, the vortex was broken up by the strong interaction between the shear layer over the cavity and the jet.

Key words: Scramjet engine, Mixing enhancement, Vortex generator, Transverse injection, Cavity, Supersonic flow
http://dx.doi.org/10.1631/jzus.A1500244 **CLC number:** V448

1 Introduction

An efficient mixing process is very important for the engineering implementation of an airbreathing propulsion system. Many mixing enhancement devices have been proposed in recent years, including transverse jet (Lee and Mitani, 2003; Huang *et al.*, 2012b; 2012c), ramp (Alexander *et al.*, 2006; Huang *et al.*, 2013b), strut (Huang *et al.*, 2011c; Sujith *et al.*, 2013), pylon (Gruenig *et al.*, 2000; Gruber *et al.*, 2008; Takahashi *et al.*, 2010; Lee, 2012; Pohlman and Greendyke, 2013), and cavity (Yu and Schadow, 1994; Huang *et al.*, 2012a; 2013a), as well as double cavities in parallel or tandem (Huang *et al.*, 2011b) and some combinations (Hsu *et al.*, 2010; Grady *et al.*, 2012). These devices can provide an axial vortex which has been proved to be responsible for improving mixing in supersonic flows.

Vergine *et al.* (2015) studied the influences of the imposed interaction and subsequent dynamics of a system of selected supersonic streamwise vortices on the reacting plume morphology and its evolution. The hydrogen plume issued from two pylon-type injectors. Huang and Yan (2013) gave a detailed review of transverse injection schemes in supersonic flows, and found that the mixing process in the transverse injection flow field is influenced by many geometric parameters, suggesting that it is a multi-objective problem. Vinogradov *et al.* (2007)

* Project supported by the National Natural Science Foundation of China (No. 11502291), and the Fund for Owner of Outstanding Doctoral Dissertation from the Ministry of Education of China (No. 201460)
ORCID: Wei HUANG, http://orcid.org/0000-0001-9805-985X

provided an overview on the pre-injection scheme involved in a pylon, and concluded that the pylon is a useful tool to enhance the mixing process in a transverse injection flow field.

The unsteadiness in the flow field produced by emission of acoustic oscillations from wall-mounted cavities has proved to be an effective tool to enhance entrainment and fuel air mixing (Das *et al.*, 2015). However, the mixing enhancement induced by a wall-mounted cavity has rarely been investigated, and the cavity is more often used to hold the flame in the scramjet engine. Yu and Schadow (1994) were the first to propose cavity based mixing phenomena. They observed that the spreading of a cavity actuated mixing layer was much higher than that of an ordinary mixing layer for the same velocity and density ratios. Handa *et al.* (2014) experimentally compared supersonic mixing fields in three ducts without any devices, with a rectangular cavity, or with the proposed cavity. They found that mixing, as well as jet penetration, was enhanced far more rapidly in the duct with the proposed cavity. This effect is induced by the large-amplitude jet fluctuation due to oscillatory secondary flows. However, detailed flow field structures and quantitative evaluation were lacking. This information should be explored further using a computational fluid dynamics approach. Recently, with the improvement in computer capability, this approach has become an efficient tool to support ground experimental tests.

In this study, three physical models were employed to investigate the supersonic mixing enhancement mechanism induced by the proposed cavity configuration, and grid discrepancy analysis was used to choose a suitable grid scale. A large eddy simulation and optimization design of these configurations, as well as a study of the combustion process, will be conducted in the near future, but this is beyond the scope of this paper.

2 Physical model and numerical approach

2.1 Physical model

The physical models have a height of 7.5 mm and a width of 42 mm at the entrance, and a section with a 3° divergence angle to avoid unstarting in the wind tunnel due to injection or boundary layer growth (Fig. 1). Fig. 1 shows the plan and symmetric views of the three physical models employed in this study, namely the conventional physical model, novel physical model I, and novel physical model II. The origin of the coordinate system is located in the centre of the middle injector. The middle injector is located in the symmetric plane of the model. For all three physical models, injection ports of 1.5 mm diameter are located 22 mm downstream of the entrance of the divergence section, and the distance between two injectors is 12 mm. These specifications are the same as those employed by Handa *et al.* (2014).

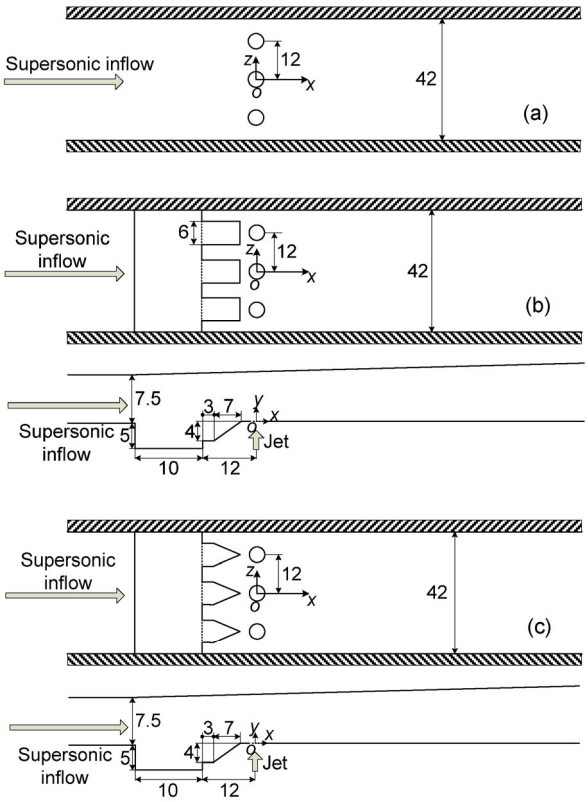

Fig. 1 Plan and symmetric views of the three physical models employed in this study: (a) conventional physical model; (b) novel physical model I; (c) novel physical model II (unit: mm)

The length and depth of the cavity mounted in novel physical models I and II are 10 mm and 5 mm, respectively, and the leading edge of the cavity is located at the entrance of the divergence section for novel physical models I and II. For novel physical models I and II, three parts of the rear face of the

cavity are cut out, and the length and width of the cut out part are 10 mm and 6 mm, respectively.

The air flows into the combustor from left to right with a static pressure of 43882.48 Pa and total temperature of 297 K. Hydrogen was used as the injectant in this study, and was injected into the combustor with sonic velocity. Its static pressure was 166863.1 Pa, and its total temperature was 297 K. The parametric distributions at the exit of the wall orifice and at the entrance of the combustor are uniform. The effect of the flow field property in the inlet on combustor performance was not considered in this study, although the incoming boundary layer thickness has a great impact on the flow inside the cavity. This information will be obtained in future work.

2.2 Numerical method

Steady state computational data were obtained using FLUENT version 6.3.26, and mesh was generated using Gambit (Fluent Inc., 2006). A Dell workstation at the Science and Technology on Scramjet Laboratory, China, using up to 32 processors, provided a parallel computing environment for flow solutions.

For this study, the 3D Reynolds-averaged Navier-Stokes (RANS) equations were solved using a coupled, implicit, second-order upwind solver. Cell fluxes were computed using an AUSM scheme and the viscosity determined using mass-weighted-mixing-law. The operational fluid was air, treated as an ideal gas with no reactions modeled.

The k-ω shear stress transport (SST) model was used for turbulence modeling. The SST model combines the advantages of the k-ω model near solid surfaces with those of the k-ε model, which has good free-shear-flow properties, making it well suited for this flow. The SST model also shows better performance than either the k-ω or k-ε models in adverse pressure gradient flows (Freeborn *et al.*, 2009). The SST model was utilized successfully in previous studies on transverse injection (Huang, 2014; 2015) and backward-facing step flows (Huang *et al.*, 2014a). The Courant-Friedrichs-Levy (CFL) number remained at 0.5 with suitable under-relaxation factors to ensure stability. No-slip conditions (u=v=w =0) were assumed for wall boundaries. At the outflow, all the physical variables were extrapolated from the internal cells based on the flow being supersonic (Kim *et al.*, 2004).

The solution was considered to have converged when most of the residuals reached their minimum values after falling more than three orders of magnitude, and the difference between the computed inflow and the outflow mass flux was required to drop below 0.005 kg/s. Fig. 2 shows the convergence history for novel physical model II, and it represents the residuals of the variable parameters, including the velocities, energy, k and ω for the turbulence model, and the species considered in the current study, namely air, H_2, and O_2. Three grid scales were employed to analyze grid independency for the conventional physical model, namely coarse grid (942703 cells), moderate grid (1200223 cells), and refined grid (1492543 cells). The grid was multi-blocked and highly concentrated close to the wall surfaces, the fuel injector, and the cavity to ensure the accuracy of the numerical simulation. Fig. 3 represents the grid system for novel physical model I, and Fig. 4 depicts a close-up view of the grid system around the cavity in novel physical model I. To show the configuration of the cavity in the flowpath, Fig. 5 shows details of the meshes at the bottom wall of the cavity. The height of the first row of cells is set at a distance

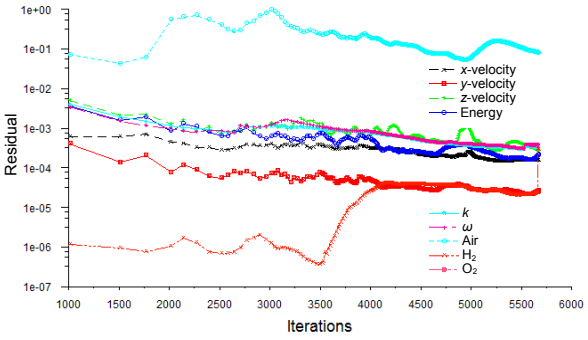

Fig. 2 Convergence history for novel physical model II

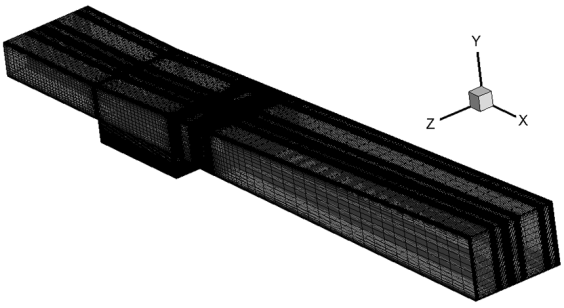

Fig. 3 Grid system for novel physical model I

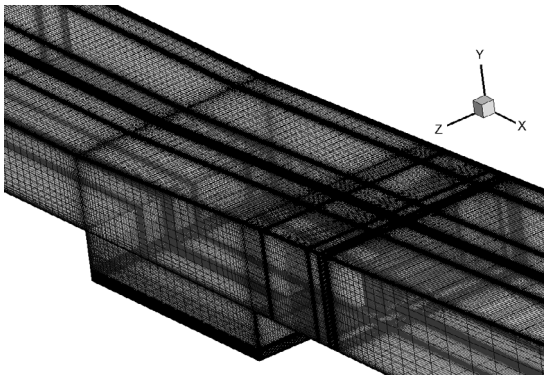

Fig. 4 Close-up view of the grid system around the cavity in novel physical model I

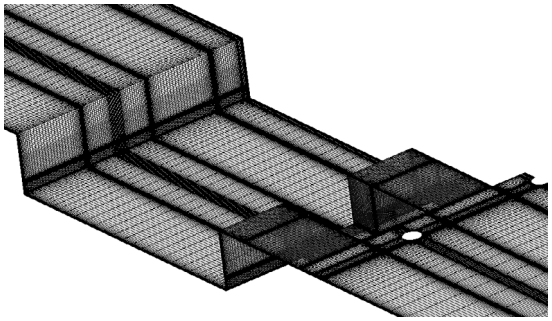

Fig. 5 Close-up view of the grid system at the bottom wall of the cavity in novel physical model I

of 0.001 mm for the walls, and the maximum wall y^+ is less than 9.1. This proved to be suitable for turbulent mixing simulation of supersonic flows (Pudsey and Boyce, 2010), as well as combustion flow field simulation in a cavity-based combustor (Huang *et al.*, 2014b).

3 Code validation and grid independency analysis

The numerical approach mentioned above has been utilized successfully to analyze the flow field in cases with a cavity (Huang *et al.*, 2011a) and with transverse injection ports (Huang, 2014). For convenience, the code validation process is not provided in this section, and readers are referred to Huang *et al.* (2011a) and Huang (2014). A comparison between numerical results and published experimental data, as well as the grid independency analysis, has been provided by Huang *et al.* (2011a) and Huang (2014).

Fig. 6 shows the effect of different grid scales on wall static pressure in the conventional physical model. The grid scale has only a slight impact on the wall static pressure distribution. The largest discrepancy occurs when x≈50 mm. The discrepancy between the results predicted by the moderate and refined grids is much smaller than that between the results predicted by the coarse and moderate grids. This may imply that the number of cells in the moderate grid system is sufficient for this investigation. The number of time steps increases with the number of grid cells to obtain a steady flow field. This is related to the parallel computing environment and the numerical method employed (Smirnov *et al.*, 2014). The accumulation of stochastic error is proportional to the number of time steps and depends on the accuracy of the scheme and the approximation error (Smirnov and Nikitin, 2014). Fig. 7 depicts a comparison of the Mach number (Ma) contours on the symmetric and four cross-sectional planes of the conventional physical model with different grid scales. The grid scale makes a slight difference to the Mach number contours as well. The Mach disk and the bow shock wave upstream of the injector are clearly captured by all three grid scales, and the core of the counter-rotating vortex pair (CVP) moves towards the upper wall with the increasing horizontal distance. Thus, 2 290 350 and 2 301 429 cells were employed for the simulations of novel physical models I and II, respectively, in the following discussion.

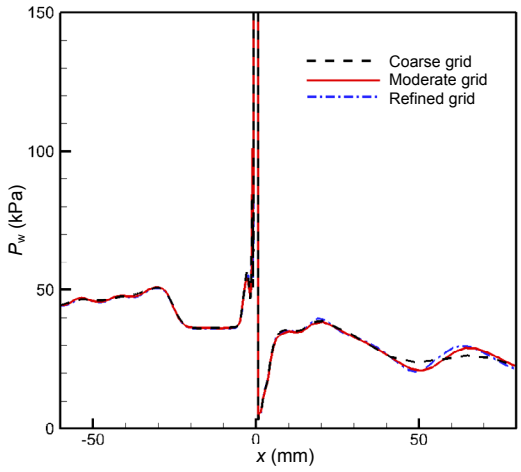

Fig. 6 Comparison of wall static pressure (P_w) resulting from different grid scales used in the conventional physical model

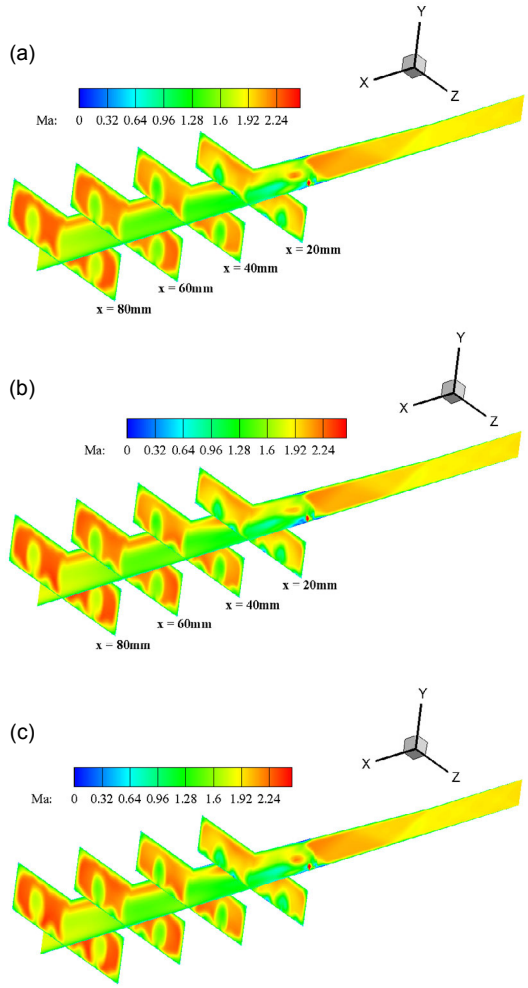

Fig. 7 Comparison of Mach number contours on the symmetric and four cross-sectional planes resulting from different grid scales used in the conventional physical model

(a) Coarse grid; (b) Moderate grid; (c) Refined grid

4 Results and discussion

Fig. 8 depicts the comparison between the Mach number contours on the symmetric and four cross-sectional planes for the three physical models with a moderate grid scale. The subsonic area of the case with the cavity is larger than that of the case with only transverse injection ports (Figs. 8b and 8c). Further, the peach-shaped vortex (Huang *et al.*, 2013b) at x=20 mm is broken up, especially for novel physical model I (Fig. 9). The mode of the flow field structure is symmetric at x=20, 40, 60, and 80 mm, and a larger separation region occurs on the top wall of the combustor. Fig. 9 compares the vortex structure at the cross-sectional plane x= 20 mm. The peach-shaped vortex generated in the core flow is clearly broken up. This may be induced by the strong interaction between the shear layer over the cavity and the jet. Also, the reflected oblique shock wave has a large impact on the augmentation of mixing of the transverse jet (Zare-Behtash *et al.*, 2015). At the same time, the case with the cavity mounting upstream of the transverse injection ports shows stronger 3D effects.

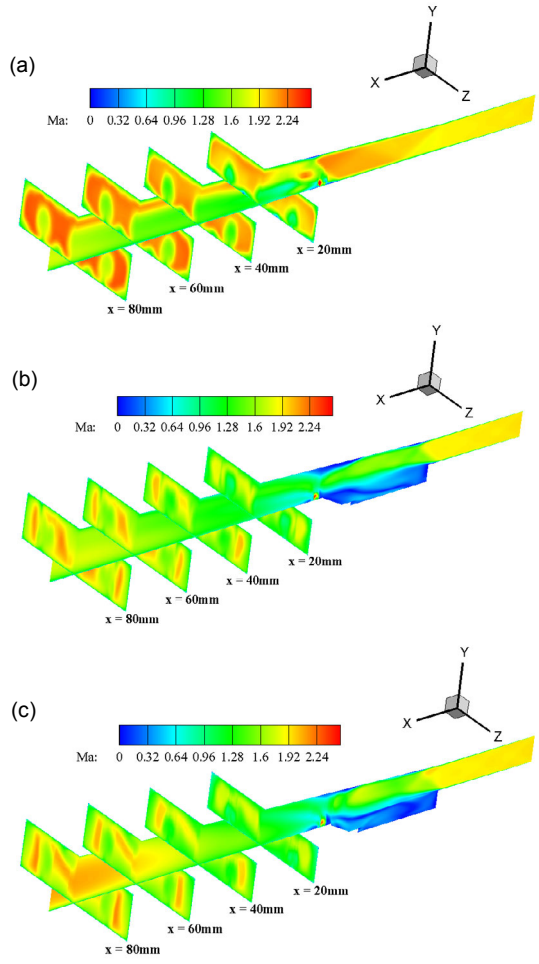

Fig. 8 Comparison of Mach number contours on the symmetric and four cross-sectional planes for three physical models with a moderate grid scale

(a) Conventional physical model; (b) Novel physical model I; (c) Novel physical model II

Fig. 10 shows a comparison of the hydrogen mole fraction contours on the symmetric and four cross-sectional planes for the three physical models

with a moderate grid scale. The vortex moves towards the top wall of the combustor due to the interaction of the shear layer over the cavity and the jet (Fig. 9). The peach-shaped vortex at the core flow is broken into small vortexes which move towards the top wall of the combustor. At the same time, the interactional effect is more serious for the middle vortex occurring on the symmetric plane (Figs. 10b and 10c). This implies that the case with the cavity is beneficial to jet penetration, especially for novel physical model II (Fig. 10c).

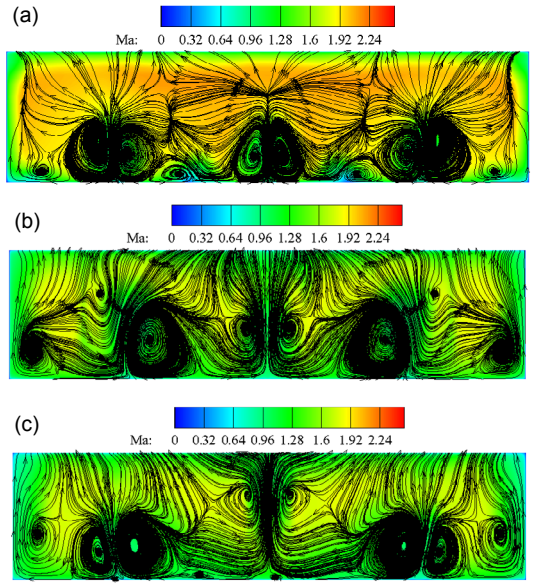

Fig. 9 Comparison of vortex structure at the cross-sectional plane x=20 mm
(a) Conventional physical model; (b) Novel physical model I; (c) Novel physical model II

To evaluate the influence of the cavity mounted upstream of the transverse injection ports on the fuel spread process, the hydrogen mole fraction contour on the lower wall of the combustor was compared (Fig. 11). Fig. 11 represents a comparison of the hydrogen mole fraction contours on the lower wall for three physical models with a moderate grid scale. Clearly, the hydrogen mole fraction is the largest for the case with only the transverse injection ports (Fig. 11a). The hydrogen mole fraction for novel physical model I is the smallest (Fig. 11b). The hydrogen injected from the middle injector for novel physical model II is away from the lower wall of the combustor (Fig. 11c), and this may imply that its mixing process is more complete and its penetration depth is larger. More fuel was wrapped into the core flow and mixed with the air stream. This result is consistent with that observed in Fig. 10c.

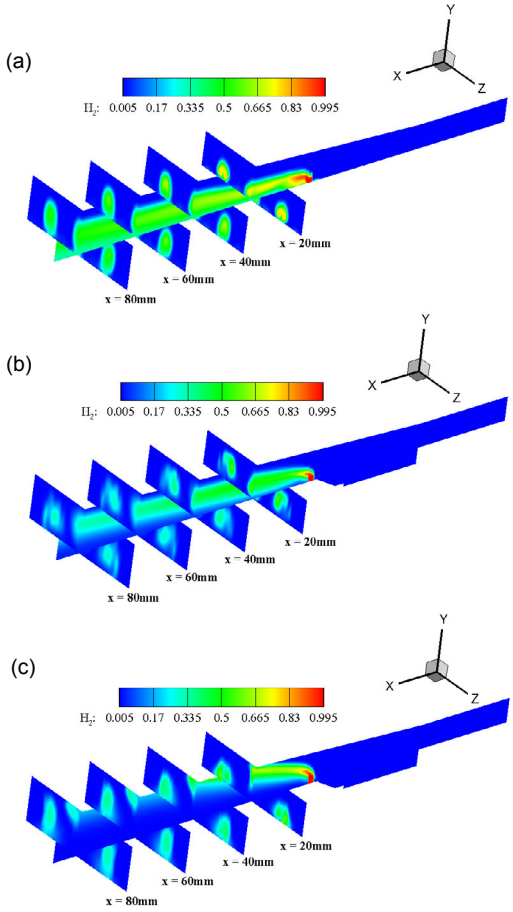

Fig. 10 Comparison of hydrogen mole fraction contours on the symmetric and four cross-sectional planes for three physical models with a moderate grid scale
(a) Conventional physical model; (b) Novel physical model I; (c) Novel physical model II

The injectant/air mixing efficiency was chosen to analyze the mixing enhancement induced by the wall-mounted cavity, and it was defined as (Segal, 2009)

$$\varphi=\frac{\dot{m}_{\text{fuel,mixed}}}{\dot{m}_{\text{fuel,total}}}=\frac{\int \alpha_{\text{react}}\rho\mu \mathrm{d}A}{\int \alpha\rho\mu \mathrm{d}A}, \tag{1}$$

$$\alpha_{\text{react}}=\begin{cases}\alpha, & \alpha\le\alpha_{\text{stoic}},\\ \alpha(1-\alpha)/(1-\alpha_{\text{stoic}}), & \alpha>\alpha_{\text{stoic}},\end{cases} \tag{2}$$

where α is the injectant mass fraction, α_{react} is the injectant fraction mixed in a proportion that reacts, α_{stoic} is the injectant stoichiometric mass fraction, $\dot{m}_{fuel,mixed}$ is the mixed injectant mass flow rate, and $\dot{m}_{fuel,total}$ is the total injectant mass flow rate. ρ and μ are the local density and velocity, respectively, and A is the cross section of the axial station where mixing is evaluated. The value for the hydrogen stoichiometric mass fraction was 0.028 31, and the cross section of the axial station varied due to the special properties of the flowpath. In this study, the mixing efficiencies at cross-sectional areas (x=20, 40, 60, and 80 mm) were evaluated and were all downstream of the jet orifice.

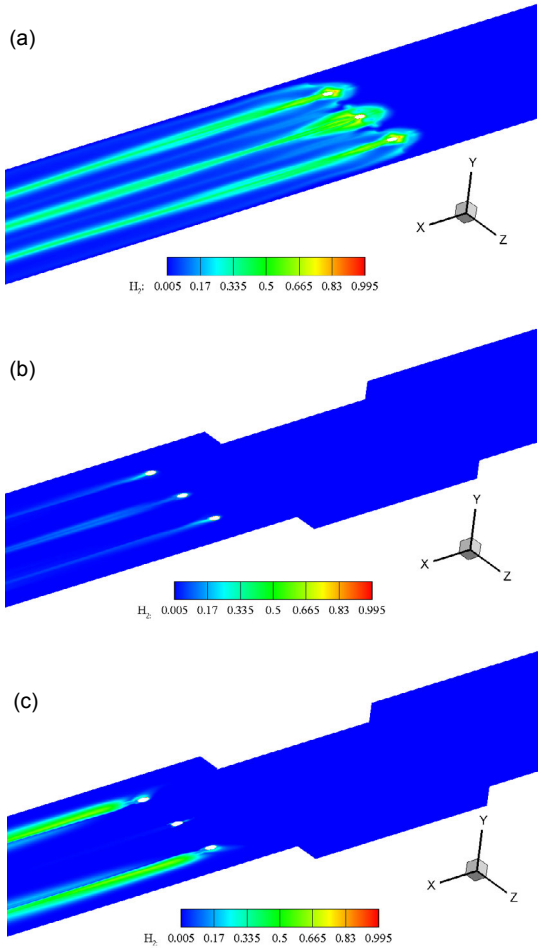

Fig. 11 Comparison of hydrogen mole fraction contours on the lower wall for three physical models with a moderate grid scale

(a) Conventional physical model; (b) Novel physical model I; (c) Novel physical model II

Fig. 12 depicts a comparison of the mixing efficiency for the physical models employed in this study. The mixing of air and injectant is enhanced by the wall-mounted cavity. Further, it is obvious that proposed novel physical model I was the best configuration for the flowpath design of the scramjet engine, and its mixing efficiency at x=40 mm was 100%. The conventional physical model without the wall-mounted cavity was the worst configuration, as the air and injectant were not mixed completely, even at the exit of the model; the mixing efficiency at x=80 mm was 98.64%, slightly lower than that of novel physical model I at x=20 mm. This further implies that the interaction between the shear layer over the cavity and the jet has a large impact on the mixing enhancement in supersonic flows.

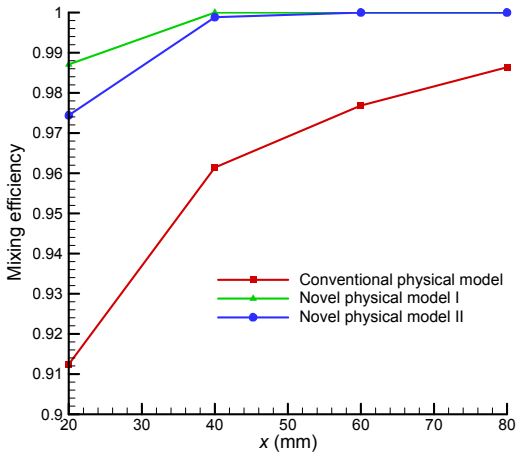

Fig. 12 Comparison of the mixing efficiency of the physical models employed in this study

5 Conclusions

In this paper, the mixing process induced by a cavity mounted upstream of the transverse injection ports was investigated numerically, and grid independency analysis was conducted. The mixing efficiencies at four cross-sectional planes, namely x=20, 40, 60, and 80 mm, were compared for the physical models employed in this study. We have come to the following conclusions:

1. In the case with only the transverse injection ports the vortex was broken up by the strong interaction between the shear layer over the cavity and the

jet. Accordingly, the area of the subsonic region was larger for the case with the cavity mounted upstream of the transverse injection ports.

2. Hydrogen penetrated deeper in the case with the cavity mounted upstream of the transverse injection ports, especially for novel physical model II. This is beneficial to the mixing process in supersonic flows.

3. Novel physical model I had the highest mixing efficiency. The strong interaction between the shear layer over the cavity and the jet has a large impact on the mixing enhancement in supersonic flows, and this is a fundamental step for the optimization of scramjet combustor configurations.

References

Alexander, D.C., Sislian, J.P., Parent, B., 2006. Hypervelocity fuel/air mixing in mixed-compression inlets of shcramejts. *AIAA Journal*, **44**(10):2145-2155. http://dx.doi.org/10.2514/1.12630

Das, R., Kim, J.S., Kim, H.D., 2015. Supersonic cavity based combustion with kerosene/hydrogen fuel. *Journal of Thermal Science*, **24**(2):164-172. http://dx.doi.org/10.1007/s11630-015-0769-z

Fluent Inc., 2006. Fluent 6.3 User's Guide. Fluent Inc., Lebanon, NH, USA.

Freeborn, A.B., King, P.I., Gruber, M.R., 2009. Swept-leading-edge pylon effects on a scramjet pylon-cavity flameholder flowfield. *Journal of Propulsion and Power*, **25**(3):571-582. http://dx.doi.org/10.2514/1.39546

Grady, N.R., Pitz, R.W., Carter, C.D., *et al.*, 2012. Supersonic flow over a ramped-wall cavity flame holder with an upstream strut. *Journal of Propulsion and Power*, **28**(5):982-990. http://dx.doi.org/10.2514/1.B34394

Gruber, M.R., Carter, C.D., Montes, D.R., *et al.*, 2008. Experimental studies of pylon-aided fuel injection into a supersonic crossflow. *Journal of Propulsion and Power*, **24**(3):460-470. http://dx.doi.org/10.2514/1.32231

Gruenig, C., Avrashkov, V., Mayinger, F., 2000. Fuel injection into a supersonic airflow by means of pylons. *Journal of Propulsion and Power*, **16**(1):29-34. http://dx.doi.org/10.2514/2.5560

Handa, T., Nakano, A., Tanigawa, K., *et al.*, 2014. Supersonic mixing enhanced by cavity-induced three-dimensional oscillatory flow. *Experiments in Fluids*, **55**:1711. http://dx.doi.org/10.1007/s00348-014-1711-y

Hsu, K.Y., Carter, C.D., Gruber, M.R., *et al.*, 2010. Experimental study of cavity-strut combustion in supersonic flow. *Journal of Propulsion and Power*, **26**(6):1237-1246. http://dx.doi.org/10.2514/1.45767

Huang, W., 2014. Design exploration of three-dimensional transverse jet in a supersonic crossflow based on data mining and multi-objective design optimization approaches. *International Journal of Hydrogen Energy*, **39**(8):3914-3925. http://dx.doi.org/10.1016/j.ijhydene.2013.12.129

Huang, W., 2015. Effect of jet-to-crossflow pressure ratio arrangement on turbulent mixing in a flowpath with square staged injectors. *Fuel*, **144**:164-170. http://dx.doi.org/10.1016/j.fuel.2014.12.051

Huang, W., Yan, L., 2013. Progress in research on mixing techniques for transverse injection flow fields in supersonic crossflows. *Journal of Zhejiang University-SCIENCE A (Applied Physics & Engineering)*, **14**(8):554-564. http://dx.doi.org/10.1631/jzus.A1300096

Huang, W., Pourkashanian, M., Ma, L., *et al.*, 2011a. Investigation on the flameholding mechanisms in supersonic flows: backward-facing step and cavity flameholder. *Journal of Visualization*, **14**(1):63-74. http://dx.doi.org/10.1007/s12650-010-0064-8

Huang, W., Wang, Z.G., Jin, L., *et al.*, 2011b. Effect of cavity location on combustion flow field of integrated hypersonic vehicle in near space. *Journal of Visualization*, **14**(4):339-351. http://dx.doi.org/10.1007/s12650-011-0100-3

Huang, W., Wang, Z.G., Luo, S.B., *et al.*, 2011c. Parametric effects on the combustion flow field of a typical strut-based scramjet combustor. *Chinese Science Bulletin*, **56**(35):3871-3877. http://dx.doi.org/10.1007/s11434-011-4823-2

Huang, W., Pourkashanian, M., Ma, L., *et al.*, 2012a. Effect of geometric parameters on the drag of the cavity flameholder based on the variance analysis method. *Aerospace Science and Technology*, **21**(1):24-30. http://dx.doi.org/10.1016/j.ast.2011.04.009

Huang, W., Liu, W.D., Li, S.B., *et al.*, 2012b. Influences of the turbulence model and the slot width on the transverse slot injection flow field in supersonic flows. *Acta Astronautica*, **73**:1-9. http://dx.doi.org/10.1016/j.actaastro.2011.12.003

Huang, W., Ma, L., Pourkashanian, M., *et al.*, 2012c. Parametric effects in a scramjet engine on the interaction between the air stream and the injection. *Proceedings of the Institution of Mechanical Engineers, Part G: Journal of Aerospace Engineering*, **226**(3):294-309. http://dx.doi.org/10.1177/0954410011408512

Huang, W., Liu, J., Yan, L., *et al.*, 2013a. Multiobjective design optimization of the performance for the cavity flameholder in supersonic flows. *Aerospace Science and Technology*, **30**(1):246-254. http://dx.doi.org/10.1016/j.ast.2013.08.009

Huang, W., Li, S.B., Yan, L., *et al.*, 2013b. Performance evaluation and parametric analysis on cantilevered ramp injector in supersonic flows. *Acta Astronautica*, **84**:141-152. http://dx.doi.org/10.1016/j.actaastro.2012.11.011

Huang, W., Jin, L., Yan, L., *et al.*, 2014a. Influence of jet-to-crossflow pressure ratio on nonreacting and reacting processes in a scramjet combustor with backward-facing steps. *International Journal of Hydrogen Energy*, **39**(36):21242-21250. http://dx.doi.org/10.1016/j.ijhydene.2014.10.073

Huang, W., Wang, Z.G., Yan, L., *et al.*, 2014b. Variation of inlet boundary conditions on the combustion characteristics of a typical cavity-base scramjet combustor. *Proceedings of the Institution of Mechanical Engineers, Part G: Journal of Aerospace Engineering*, **228**(4):627-638. http://dx.doi.org/10.1177/0954410013480076

Kim, K.M., Baek, S.W., Han, C.Y., 2004. Numerical study on supersonic combustion with cavity-based fuel injection. *International Journal of Heat and Mass Transfer*, **47**(2):271-286. http://dx.doi.org/10.1016/j.ijheatmasstransfer.2003.07.004

Lee, S.H., 2012. Mixing augmentation with cooled pylon injection in a scramjet combustor. *Journal of Propulsion and Power*, **28**(3):477-485. http://dx.doi.org/10.2514/1.B34220

Lee, S.H., Mitani, T., 2003. Mixing augmentation of transverse injection in scramjet combustor. *Journal of Propulsion and Power*, **19**(1):115-124. http://dx.doi.org/10.2514/2.6087

Pohlman, M.R., Greendyke, R.B., 2013. Parametric analysis of pylon-aided fuel injection in scramjet engines. *Journal of Engineering for Gas Turbines and Power*, **135**(2):024501. http://dx.doi.org/10.1115/1.4007735

Pudsey, A.S., Boyce, R.R., 2010. Numerical investigation of transverse jets through multiport injector arrays in supersonic crossflow. *Journal of Propulsion and Power*, **26**(6):1225-1236. http://dx.doi.org/10.2514/1.39603

Segal, C., 2009. The Scramjet Engine: Processes and Characteristics. Cambridge University Press, UK. http://dx.doi.org/10.1017/CBO9780511627019

Smirnov, N.N., Nikitin, V.F., 2014. Modeling and simulation of hydrogen combustion in engines. *International Journal of Hydrogen Energy*, **39**(2):1122-1136. http://dx.doi.org/10.1016/j.ijhydene.2013.10.097

Smirnov, N.N., Betelin, V.B., Shagaliev, R.M., *et al.*, 2014. Hydrogen fuel rocket engines simulation using LOGOS code. *International Journal of Hydrogen Energy*, **39**(20):10748-10756. http://dx.doi.org/10.1016/j.ijhydene.2014.04.150

Sujith, S., Muruganandam, T.M., Kurian, J., 2013. Effect of trailing ramp angles in strut-based injection in supersonic flow. *Journal of Propulsion and Power*, **29**(1):66-78. http://dx.doi.org/10.2514/1.B34532

Takahashi, H., Tu, Q., Segal, C., 2010. Effects of pylon-aided fuel injection on mixing in a supersonic flowfield. *Journal of Propulsion and Power*, **26**(5):1092-1101. http://dx.doi.org/10.2514/1.48393

Vergine, F., Crisanti, M., Maddalena, L., 2015. Supersonic combustion of pylon-injected hydrogen in high-enthalpy flow with imposed vortex dynamics. *Journal of Propulsion and Power*, **31**(1):89-103. http://dx.doi.org/10.2514/1.B35330

Vinogradov, V.A., Shikhman, Y.M., Segal, C., 2007. A review of fuel pre-injection in supersonic, chemically reacting flows. *Applied Mechanics Reviews*, **60**(4):139-148. http://dx.doi.org/10.1115/1.2750346

Yu, K.H., Schadow, K.C., 1994. Cavity-actuated supersonic mixing and combustion control. *Combustion and Flame*, **99**(2):295-301. http://dx.doi.org/10.1016/0010-2180(94)90134-1

Zare-Behtash, H., Lo, K.H., Kontis, K., *et al.*, 2015. Transverse jet-cavity interactions with the influence of an impinging shock. *International Journal of Heat and Fluid Flow*, **53**:146-155. http://dx.doi.org/10.1016/j.ijheatfluidflow.2015.03.004

中文概要

题　目：壁面凹腔诱导的超声速混合增强机制研究

目　的：探索壁面凹腔诱导下的超声速混合增强机理，期望得到混合性能较好的燃料喷注策略。

方　法：提出两种壁面凹腔与横向射流的组合方式，采用数值模拟方法对其流场进行研究，并与纯横向射流流场细节进行对比。

结　论：1. 由于凹腔上面剪切层与壁面横向射流的强烈交互作用，使得横向射流流场中产生的涡系结构被打破；相应地，当把凹腔置于喷孔上游时，亚声速区域面积更大；2. 当把凹腔置于喷孔上游时，燃料的渗透深度更大，这样有利于超声速气流中燃料与空气的混合；3. 新构型 I 的混合效率最高。凹腔上面剪切层与壁面横向射流之间的强烈交互作用对超声速气流中燃料的混合增强影响很大，这是超燃冲压发动机燃烧室构型优化的基石。

关键词：超燃冲压发动机；混合增强；涡流发生器；横向射流；凹腔；超声速气流